Naval Research Laboratory
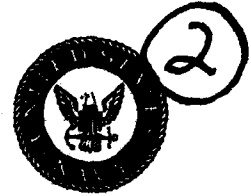
Washington, DC 20375-5000

NRL Report 9132

AD-A199 950

Adaptive Phase-Shifter Nulling Techniques for Large-Aperture Phased Arrays

W. F. GABRIEL*

Electromagnetics Branch
Radar Division

Sachs/Freeman Associates, Inc.
Landover, MD 20785

August 15, 1988

88 10 5 198

REPORT DOCUMENTATION PAGE

Form Approved
OMB No 0704 0188

1a REPORT SECURITY CLASSIFICATION UNCLASSIFIED		1b RESTRICTIVE MARKINGS			
2a SECURITY CLASSIFICATION AUTHORITY		3 DISTRIBUTION AVAILABILITY OF REPORT			
2b DECLASSIFICATION / DOWNGRADING SCHEDULE		Approved for public release; distribution is unlimited.			
4 PERFORMING ORGANIZATION REPORT NUMBER(S) NRL Report 9132		5 MONITORING ORGANIZATION REPORT NUMBER(S)			
6a NAME OF PERFORMING ORGANIZATION Naval Research Laboratory	6b OFFICE SYMBOL (If applicable) 5370	7a NAME OF MONITORING ORGANIZATION			
6c ADDRESS (City, State, and ZIP Code) Washington, DC 20375-5000		7b ADDRESS (City State, and ZIP Code)			
8a NAME OF FUNDING / SPONSORING ORGANIZATION Naval Surface Weapons Center	8b OFFICE SYMBOL (If applicable)	9 PROCUREMENT INSTRUMENT IDENTIFICATION NUMBER			
8c ADDRESS (City, State, and ZIP Code) Silver Spring, MD 20903-5000		10 SOURCE OF FUNDING NUMBERS			
		PROGRAM ELEMENT NO 64307N	PROJECT NO S1337	TASK NO	WORK UNIT ACCESSION NO DN155-665

11 TITLE (Include Security Classification)

Adaptive Phase-Shifter Nulling Techniques for Large-Aperture Phased Arrays

12 PERSONAL AUTHOR(S)
Gabriel,* W. F.

13a TYPE OF REPORT Interim	13b TIME COVERED FROM ___ TO ___	14 DATE OF REPORT (Year, Month, Day) 1988 August 15	15 PAGE COUNT 25

17	COSATI CODES		18 SUBJECT TERMS (Continue on reverse if necessary and identify by block number)
FIELD	GROUP	SUB-GROUP	Antennas Adaptive
			Arrays Sidelobe cancelling

19 ABSTRACT (Continue on reverse if necessary and identify by block number)

Several simple phase-shifter nulling techniques are investigated for application to large-aperture phased arrays to provide a modest, partial adaptive capability at reasonable cost. These techniques do not require auxiliary elements, correlators, or beamformers, but they do require access to the array element phase shifters for injection of small phase perturbations. They also require a priori knowledge of interference source directions to facilitate fast cancellation. Particular aperture ripple modulation algorithms, based on beamspace decomposition principles and adaptive "search" techniques, are described and applied to computer simulated source situations. For example, by using a 16 element linear array, two strong sources of 5% bandwidth were nulled out within about 600 snapshots (range bins) of data; this is remarkably fast for such a simple phase-only adaptive system. The performance results achieved indicate that the concept is feasible and ready for experimental phased-array verification.

20 DISTRIBUTION / AVAILABILITY OF ABSTRACT ☒ UNCLASSIFIED/UNLIMITED ☐ SAME AS RPT ☐ DTIC USERS	21 ABSTRACT SECURITY CLASSIFICATION UNCLASSIFIED	
22a NAME OF RESPONSIBLE INDIVIDUAL W. F. Gabriel	22b TELEPHONE (Include Area Code) (202) 767-2584	22c OFFICE SYMBOL 5370

DD Form 1473, JUN 86   Previous editions are obsolete   SECURITY CLASSIFICATION OF THIS PAGE

CONTENTS

DTIC
COPY
INSPECTED
6

A-1

ADAPTIVE PHASE-SHIFTER NULLING TECHNIQUES FOR LARGE-APERTURE PHASED ARRAYS

1.0 INTRODUCTION

The particular type of antenna system addressed is a large aperture (in wavelengths) phased array of low-sidelobe design where the investment is already considerable and one simply could not afford to make it fully adaptive. The Rome Air Development Center (RADC) space-based radar (SBR) antenna system concept [1] is an excellent application case in point. The low sidelobes are necessary for good initial protection against sidelobe interference and large clutter returns. Also, they reduce the problems associated with strong sources, i.e., the number of adaptive degrees-of-freedom (DOF) required and the dynamic range of the adaptive processor. Thus, retention of the low sidelobes is considered a major requirement for the system.

Several partially adaptive array techniques are suggested in the literature for approaching this problem, including the conventional sidelobe-canceller (SLC) configuration [2,3], constrained beam-space adaptive systems [4-8], overlapped subarray (space-fed lens) configurations [1,9-11], and phase-shifter nulling techniques [12-14]. A brief commentary on each of these solutions follows.

1.1 Conventional SLC

Figure 1 illustrates the conventional SLC configuration consisting of a high-gain mainbeam antenna surrounded by an auxiliary array of a few low-gain elements. This configuration has proven popular over the years because it can provide modest protection against sidelobe interference for the least cost, with the cost being roughly proportional to the number of DOF implemented. For our purposes, the SLC concept is economically attractive as a starting point; however the specific arrangement of Fig. 1 has drawbacks because the auxiliary array is separate from the mainbeam antenna and because it operates in element space. These make it virtually impossible to achieve low adaptive sidelobes because of the inherently wide element pattern coverage, the presence of array configuration grating lobes, and the differing polarization responses. Consider the two SLC auxiliary pattern options indicated in Fig. 2, where we show cancellation of a single emitter by means of a single auxiliary element (dashed lines) and a single auxiliary beam (solid lines). Note that the emitter is nulled out by either option, but the adapted pattern sidelobe effects are quite different. The auxiliary SLC beam has little effect on the remainder of the adapted pattern sidelobes because of its highly localized interaction beamwidth region, whereas the auxiliary SLC element interacts across the entire adapted pattern sidelobe region because of its broad element pattern. In general, the auxiliary elements option produces increasing adaptive sidelobe degradation as the number of interference sources increases. Also, there can be a significant reduction in output signal-to-noise ratio (SNR) because of coupling-in additional receiver noise along with the auxiliary element signals [2].

1.2 Constrained Beamspace Antenna Systems

Many different possible configurations are within this category. Figure 3 is a schematic diagram of one particular type of constrained beamspace system [15]. It consists of two beamformer subsystems that connect into common array aperture elements. The use of common elements helps to avoid
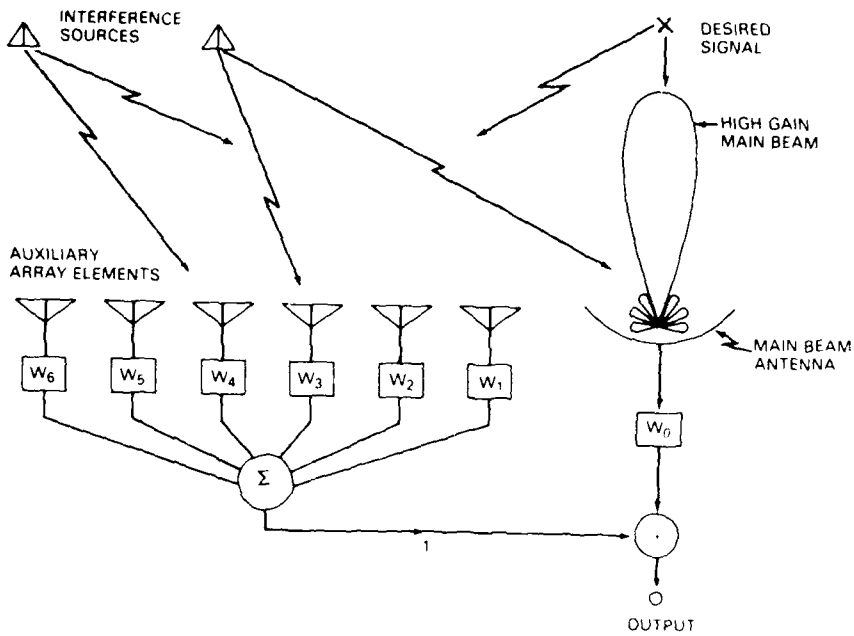
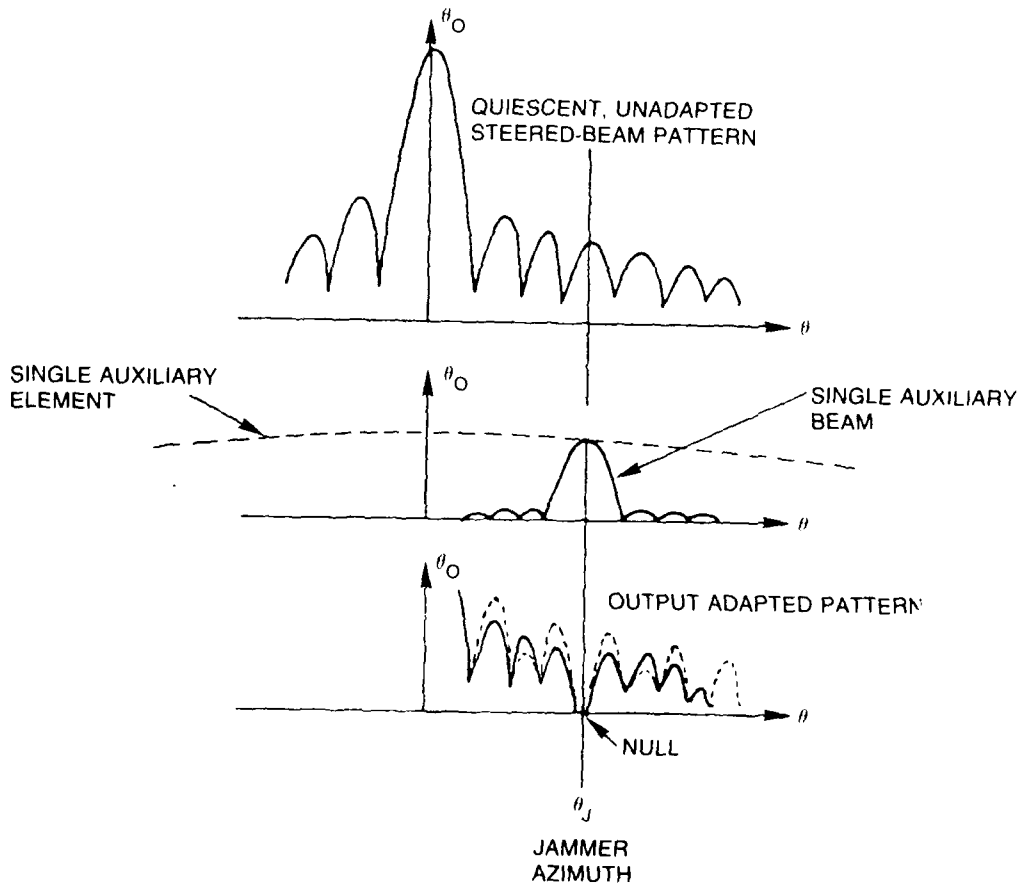Fig. 1 — Conventional adaptive side-lobe-canceller (SLC) configuration

Fig. 2 — Conceptual cancellation comparison between a single
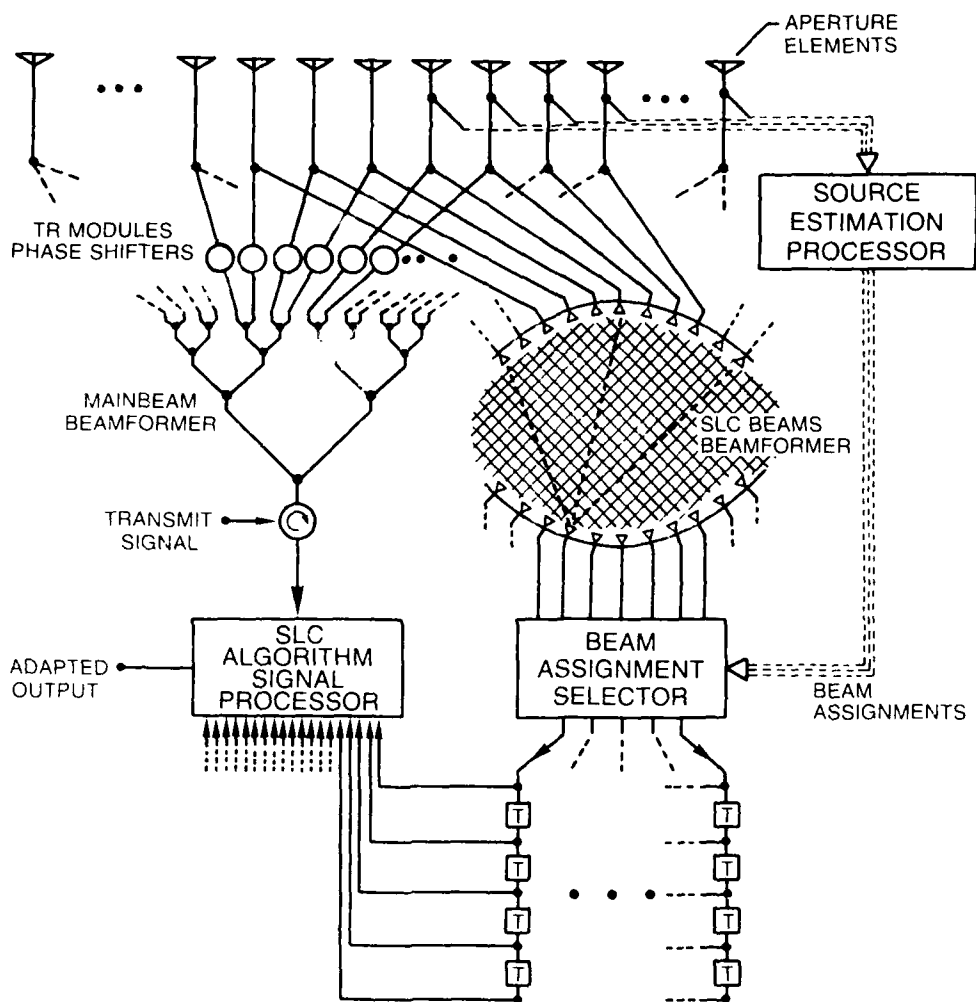auxiliary element and a single auxiliary beam

2

Fig. 3 — Constrained-beamspace SLC system with a tapped delay line on each assigned beam

polarization problems in the adaptive nulling performance. The mainbeam subsystem (on the left-hand side in Fig. 3) is intended to function as a conventional low-sidelobe phased array capable of electronic scan over the region of interest. Sidelobe level is determined by the usual quality of the elements, phase-shifter modules, and corporate feed. The second beamformer subsystem is intended to furnish a set of SLC beams for selective subtraction from the mainbeam; thus it is referred to as the SLC subsystem. This SLC subsystem is auxiliary to the mainbeam subsystem and consists of a beamformer that is coupled into the aperture at the elements prior to the transmit-receive (TR) module phase shifters. This beamformer does not require low-sidelobe design and may consist of either a Butler matrix type or a lens type, such as a Rotman lens. From the standpoint of potential bandwidth, a favorable feature is that all beams have the same phase center, i.e., the geometric center of the array aperture. Orthogonality in the family of beams is desirable but need not be precise for our purposes.

The output beam ports connect into a "Beam Assignment Selector" where they are electronically switched into the SLC algorithm processor based on source location estimates. The idea is to connect only enough SLC beams to cancel a given source distribution situation, thus minimizing

sidelobe degradation. The general principles of beamspace SLC are described in the literature [4] and offer advantages of a stable mainbeam, retention of low sidelobes, very fast adaptive response, and no adaptive grating lobes.

Each of the selected beams feeds into a tapped delay line, usually referred to as a transversal filter (TF). This arrangement permits adaptivity in the time/frequency domain [15,16] in addition to adaptivity in the spatial domain. The TF output taps then feed into the black box labeled "SLC Algorithm Signal Processor," which applies an adaptive algorithm to obtain the TR tap weights for achieving cancellation. This type of system is amenable to any of the current adaptive processing algorithms, including analog versions.

Figure 4 shows typical patterns obtained from computer simulations for a 16 element linear array. The mainbeam subsystem is given a quiescent Taylor illumination designed for 30 dB sidelobes, and a Butler matrix was chosen for the SLC subsystem beamformer. A two-beam cluster consisting of SLC beams numbers 10 and 11 were assigned to cover two strong 40 dB noncoherent sources located at 18° and 22° azimuth. Note that the adapted pattern shows cancellation of both sources with little perturbation of the mainbeam sidelobes, except in the immediate vicinity of the sources.

Figure 3 indicates that a third subsystem is the source estimation processor. This is an all-digital processor that operates on the signals received from a few of the aperture elements to detect and track the interference sources of interest. Processing the digital signals to estimate the sources may be accomplished with a number of spectral estimation algorithms available in the literature [4]. Once the source estimation information is available, we assign beamformer beams by means of a computer-logic program. It is important to note that beam assignment does not require great accuracy, i.e., a half-beamwidth is usually close enough. Also, clusters of two or three adjacent beams may be assigned for doubtful cases.

1.3 Overlapped Subarray Antenna Systems

As in the previous category, there are many possible configurations within overlapped subarray antenna systems. The type chosen for illustration is taken from Southall and McGrath [1], where Fig. 5 shows the antenna layout drawing for a completely overlapped subarray antenna (COSA). It consists of a space-fed, two-dimensional bootlace lens system in which the space-feed is a Rotman lens beamformer [17]. Figure 6(a) illustrates excitation of one of the beamformer inputs, or subarray ports, resulting in a $\sin(x)/x$ illumination of the bootlace lens. The bootlace lens, in turn, then transforms its illumination into a near-rectangular far-field pattern function that may be scanned by phase shifters behind the objective len's front face. Figure 6(b) illustrates how all of the subarray ports may be driven simultaneously (the resulting illuminations on the objective lens completely overlap one another) and are coherently combined and weighted to synthesize a tapered illumination on the objective lens, thereby producing a low sidelobe far-field pattern. Because of the Fourier transform principles of operation, this type of space-feed is often referred to as a transform feed.

A distinct advantage permitted by this type of antenna system is wide instanteous bandwidth [9], obtained by applying the appropriate time delays at subarray ports. Note that the number of time delays required in the transform feed is far less than the number that would be required to time-delay steer the objective lens, and yet it can synthesize an approximate equivalent time-delay steering over considerable bandwidth.

Since the subarray phase centers are located many wavelengths apart, the objective-lens aperture array factor contains grating lobes as illustrated in Fig. 7. The resultant overall far-field pattern is the
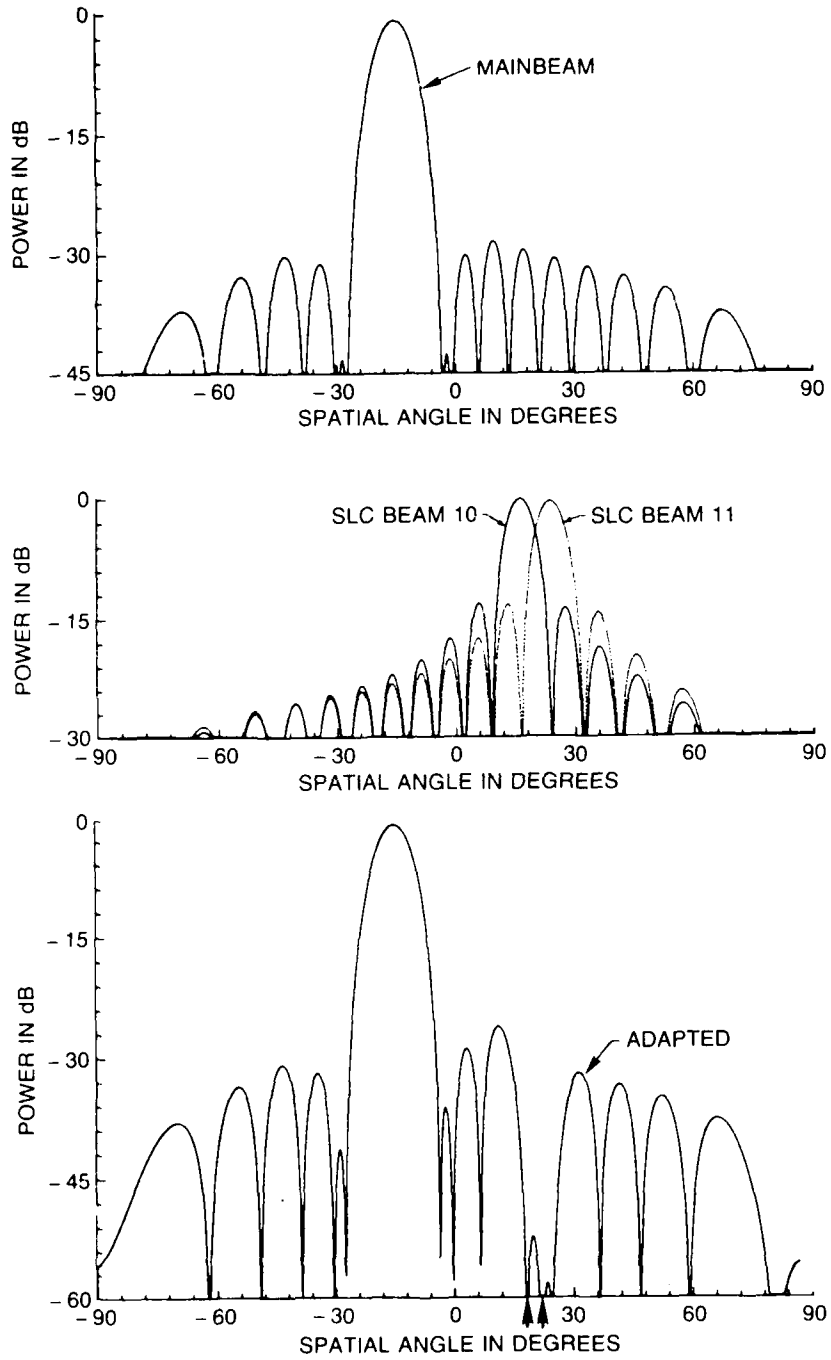
4

Fig. 4 — Patterns associated with cluster of two SLC beams, Numbers 10
and 11 assigned to two 40 dB sources at 18° and 22°
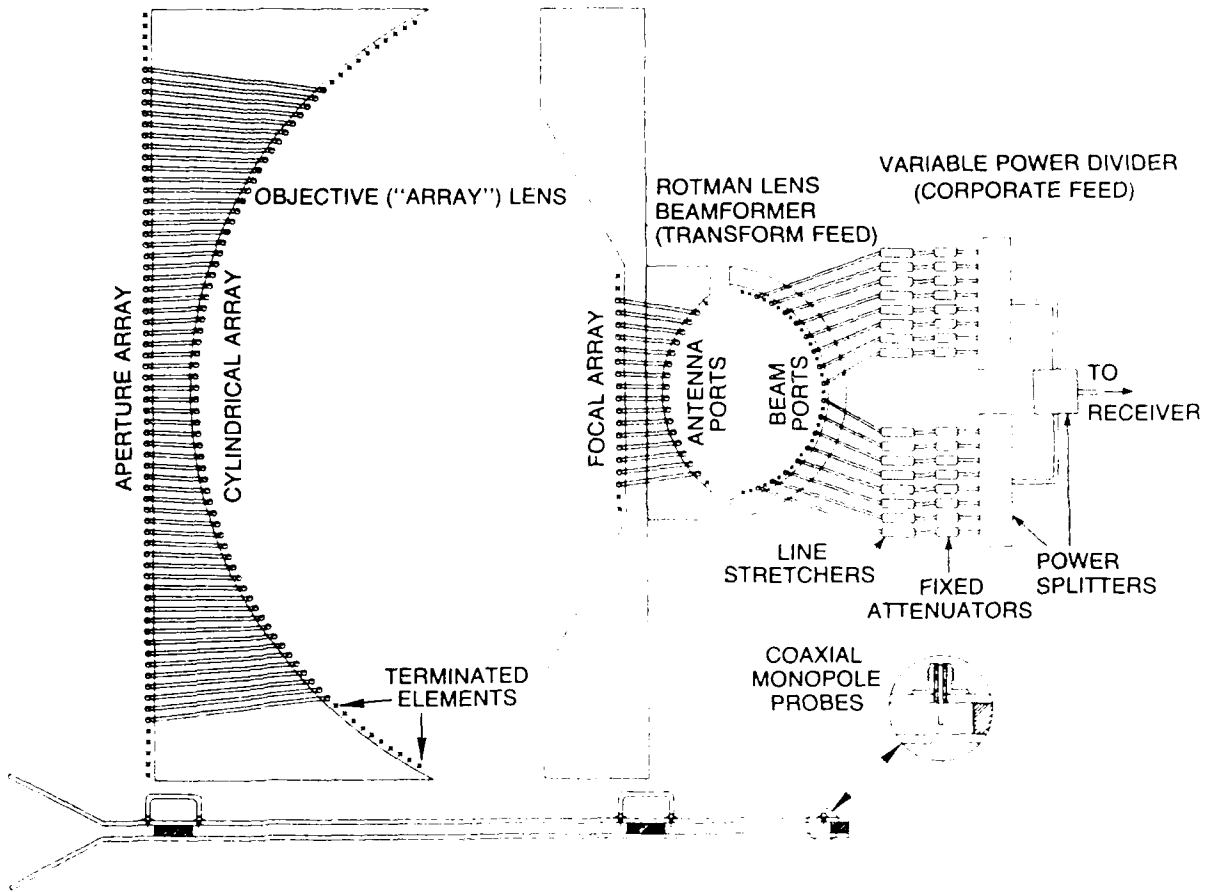
Fig. 5 — Antenna layout drawing of COSA system (Ref. 1, p. 468)

FAR FIELD PATTERN

SYNTHESIZED APERTURE TAPER

OBJECTIVE LENS

BEAMFORMER

SUBARRAY (BEAM) PORTS

AMPLITUDE WEIGHTS

(a)   (b)

Fig. 6 — COSA fundamental operating principles; (a) single subarray beam, and (b) weighted sum of subarray beams (Ref. 1, p. 466)

ARRAY PATTERN   SUBARRAY WINDOW   GRATING LOBE

$S_0 - 1/R$ $\dfrac{S_0}{R} - \gamma$ S_0 $\dfrac{S_0}{R} + \gamma$ $S_0 + 1/R$

(a)

$f > f_0$

(b)

$f < f_0$

(c)

Fig. 7 — COSA pattern characteristics; (a) $f = f_0$; (b) $f > f_0$; and (c) $f < f_0$ (Ref. 1, p. 466)

7

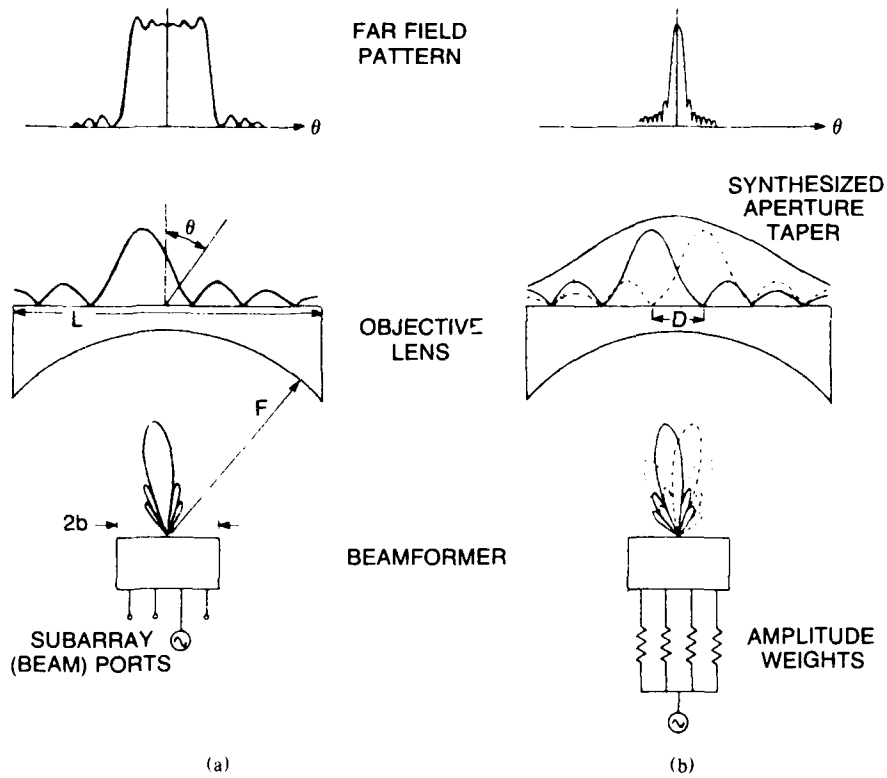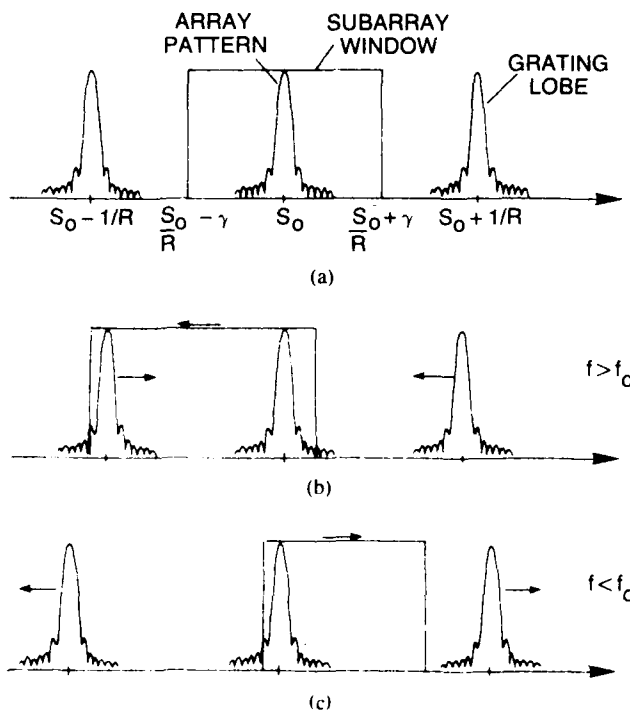product of this array factor and the flat-topped subarray pattern. The subarray pattern can be considered as a window that selects the array factor mainlobe at a given steering direction and suppresses all grating lobes. System bandwidth is eventually limited by the fact that the subarray pattern is phase-steered and shifts in angle vs frequency as illustrated in Fig. 7. Also, although the array factor mainlobe remains fixed because of its time-delay steering, all grating lobes shift in angle vs frequency and may abet intrusion into the shifting subarray window.

From a partially adaptive antenna point of view, this configuration offers three basic adaptive control alternatives:

- The subarray input-beam ports on the transform feed.

- The focal-plane-element radiators on the transform feed.

- The objective lens element phase-shifters and/or element transceiver modules.

It is beyond the scope of this report to consider these alternatives in depth because of the complexity of the systems. However, one can make some general observations based on Figs. 5, 6, and 7. The first alternative would require the fewest adaptive-weight DOF and should enable excellent adaptive performance within the confines of the flat-topped subarray pattern, i.e., in the "near-in" sidelobe region. Outside of the subarray pattern (in the "far-out" sidelobe region), adaptive performance is inferior because of low gain conditions and a severe coupled disturbance into the "near-in" sidelobe region, i.e., the entire subarray pattern must fluctuate in accordance with adaptive weight fluctuations. Mainbeam and/or sidelobe level adaptive constraints are required to prevent excessive perturbations from "far-out" sidelobe interference.

The second alternative has performance characteristics similar to the first, since they are related by a linear transformation. However, some differences are possible because of the change in objective lens illumination per adaptive weight, i.e., each adaptive weight now controls a pencil beam in the far field. One could consider certain combinations of amplitude-only and phase-only adaptive control that may be more economical than the first alternative.

The third alternative should enable the best "far-out" sidelobe region adaptive performance because its adaptive DOF can be designed to cover the entire sidelobe region of interest, even when the objective lens aperture is divided into a reasonable number of subarray "elements." Mainbeam constraints should not be required. Note, however, that this alternative is susceptible to bandwidth degradation and the hardware cost will be higher because of signal acquisition transfer complexity. Signals from the adaptively controlled subarray "elements" must be acquired and transferred from the lens to the receiver-processor. Then the resultant control signals from the receiver-processor are sent back to the lens and distributed among the elements.

1.4 Phase-Shifter Nulling Techniques

The particular configuration within this category chosen for discussion is patterned after Baird and Rassweiler [12]. When combined with simple adaptive search algorithms, this nulling method is the most simple and least expensive of all adaptive techniques available. It does not require auxiliary elements, correlators, or beamformers but depends on access to the array element phase shifters for injection of small phase (and/or amplitude) perturbations of the mainbeam-aperture distribution. Figure 8 shows a typical element-vector perturbation diagram for a phased-array antenna that uses ferrite phase shifters. One may view the perturbation as resulting from superposition of the wavefront for the mainbeam plus a wavefront for the emitter direction. Basic principles of aperture ripple-

modulation effects are described in Ref. 18, and beamspace decomposition for low-sidelobe phased arrays is described in Ref. 12.

The small phase (and/or amplitude) perturbations illustrated in Fig. 8 may be injected by means of several techniques, depending upon the particular type of components and control hardware/software available:

- The phase shifter itself may permit small analog vernier control, i.e., analog ferrite phase shifters, or even digital phase shifters in which one of the bits may be perturbed by vernier analog current drive.

- If the array contains hundreds or thousands of elements, the technique of "row/column" averaging may be used to get small, net, phase perturbations in azimuth or elevation, even though the individual phase shifters have only four- or five-bit control.

- The addition of a vernier attenuator or phase shifter at each element.

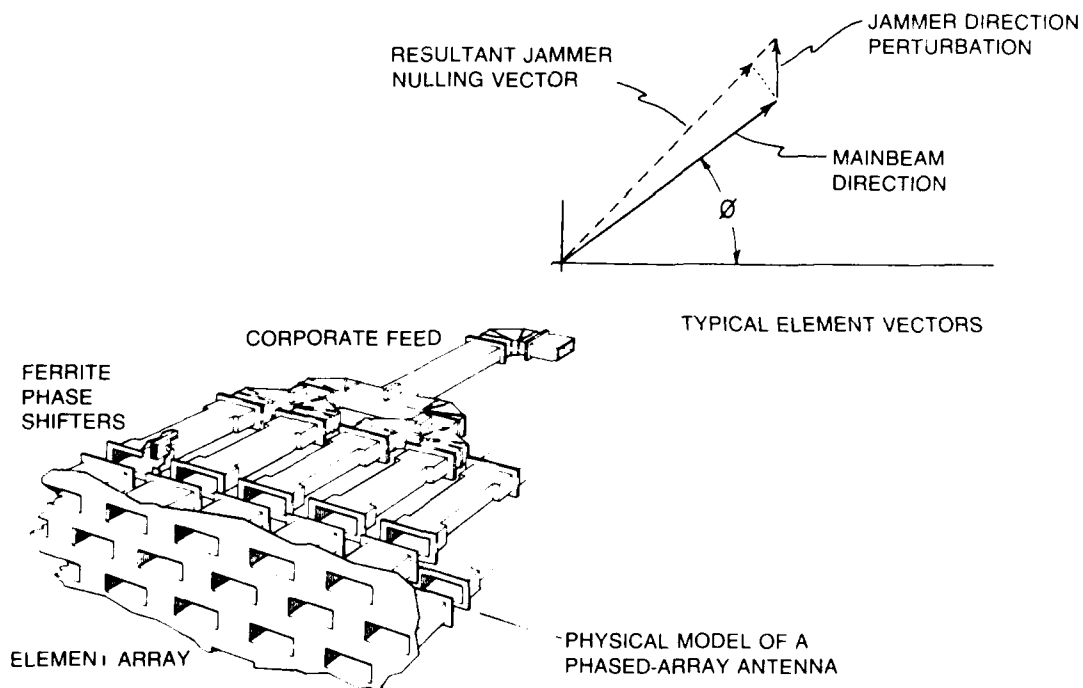- The existence of a separate, controlled beamformer coupled into the aperture elements.

Fig. 8 — Typical element vector perturbation for a phased array

The adaptive algorithms needed for adjusting the element weight perturbations are generally known as "search techniques" [13,16], and they involve using the value of some performance criteria (usually mainbeam output power) to determine the direction of the next perturbation. This class of algorithm is usually characterized by relatively slow convergence speed since individual element direction gradients are not available and must be approximated by means of time-consuming random trials. However, in the current application where we know the direction of the emitters, their relative power levels, and the mainbeam characteristics, beamspace decomposition search techniques can steer

sidelobe nulls onto the emitter positions with surprising convergence speed. This report examines this latter technique in some detail to gain a better perspective of its performance/cost tradeoff characteristics when applied to large phased-array antenna systems.

Section 2 develops the aperture ripple modulation algorithms that were used in this investigation; Section 3 discusses simulation results based on those algorithms; Section 4 presents beamspace options for improving performance at the cost of the additional DOF, and Section 5 presents the conclusions reached in this study.

2.0 APERTURE RIPPLE MODULATION ALGORITHMS

The beamspace decomposition discussed by Baird and Rassweiler [12] assumes that the source direction angles are known, whereupon we are working with the simple element vector diagram illustrated in Fig. 8. This diagram represents the superposition of the element phasing for our quiescent mainbeam wavefront, plus the phasing for each of I emitter small-amplitude wavefronts. Thus. by referring to the vector diagram, a mathematical expression may be written for the kth element weight $W(k)$ of a linear array.

$$W(k) = W_q(k) \left[1 + \sum_{i=1}^{I} A_i \exp(\psi_i(k)) \right].$$

(1)

where

$W_q(k)$ is the quiescent beam kth element weight.
A_i is the amplitude of the ith source perturbation, and
$\psi_i(k)$ is the phase of the ith source perturbation at the kth element.

Further. $\psi_i(k)$ is referenced to the quiescent-mainbeam direction element phasing and may be expanded in the form

$$\psi_i(k) = \frac{2\pi d}{\lambda} (\sin\theta_i - \sin\theta_0) \left[k - \left[\frac{K+1}{2} \right] \right].$$

(2)

where

d is the element spacing,
λ is the wavelength,
K is the total number of elements,
θ_0 is the quiescent mainbeam steering direction, and
θ_i is the direction angle of the ith source.

The array elements are assumed to be equally spaced, and all element phasing is referenced to the midpoint, or center, of the array.

The only unknown quantity in Eqs. (1) and (2) is the coefficient A_i of the small-amplitude source wavefronts. These coefficients are arrived at by a recursive modulation trial-and-update routine that may be expressed in the form,

$$A_i(n+1) = \left(\frac{\tau(n)}{\tau(n)+1} \right) A_i(n) + \mu_i(n),$$

(3)

where

$A_i(n)$ is the value of A_i used in current trial,

$A_i(n + 1)$ is the new value of A_i for the next trial,

$\mu_i(n)$ is the update increment from current trial, and

$\tau(n)$ is the integration time constant.

Note that the A_i are quantities that are formed by integrating the update increments, and that they incorporate a decay factor determined by the time constant $\tau(n)$. This time constant is chosen to have a SNR dependency as follows,

$$\tau(n) = 7.5 + \left[\frac{80}{\sqrt{S(n)}} \right], \tag{4}$$

where $S(n)$ is the current trial value of best SNR.

The update increments are determined from a weight perturbation modulation trial that involves a simple plus-minus sequence, with the array output power $P(t)$, monitored and averaged for equal time periods during the modulation trial. The sequence proceeds as follows:

Step 1:   If this is a new start, a value of averaged $P(t)$ for unperturbed weights $\mathbf{W}$ is required. Let P_0 represent that measured average power level. Note that $\mathbf{W}$ may be the quiescent mainbeam weights $\mathbf{W}_q$ if the initial A_i are set to zero for a new start (Eq. (1)).

Step 2:   If this is a new start, an initial value for the weight perturbation magnitudes Δ_i is required. Initial magnitudes are usually chosen about 6 dB below the quiescent beam sidelobe level. For example, if the nominal sidelobe level is -30 dB, then we would set the initial values of all $\Delta_i = 0.017$, or -36 dB level.

Step 3:   The Δ_i are applied as a weight perturbation modulation in plus-minus sequence for the ith source alone, where

$$W_i^+(k) = W(k)[1 + \Delta_i \exp(\psi_i(k))], \tag{5}$$

and

$$W_i^-(k) = W(k)[1 - \Delta_i \exp(\psi_i(k))], \tag{6}$$

where $\psi_i(k)$ was given in Eq. (2). The output power is monitored for this sequence, giving us two averaged power levels,

$\hat{P}_i(+)$ is the averaged $P(t)$ for $\mathbf{W}_i^+$ weights, and

$\hat{P}_i(-)$ is the averaged $P(t)$ for $\mathbf{W}_i^-$ weights.

Note that the phase term $\psi_i(k)$ confines the modulation to a particular source; we are essentially adding and subtracting a low-level beam pointed in the direction of the ith source alone. *This is a beamspace low-level modulation technique.*

11

Step 4: Determine best Δ_i from the modulation trial of Step 3. The following logic procedure is used in a Fortran IV software program:

$F = 0$

IF $((\hat{P}_i(+) > \hat{P}_0).$ AND. $(\hat{P}_i(-) > \hat{P}_0))\ F = 1$; set flag.

IF $(F = 1)$ GO TO 33   ; source in null, do not change.

$u = +1$

$X = \hat{P}_i(+) - \hat{P}_i(-)$; modulation difference in power level.

IF $(X > 0)$ GO TO 10

$Z = \hat{P}_0/\hat{P}_i(+)$; power level change ratio.

$\hat{P}_0 = \hat{P}_i(+)$; $\hat{P}_0$ ratchet-down to lowest power level.

GO TO 15

10 $u = -1$

$Z = \hat{P}_0/\hat{P}_i(-)$; power level change ratio.

$\hat{P}_0 = \hat{P}_i(-)$; $\hat{P}_0$ ratchet-down to lowest power level.

15 $\mu_i(n) = u * \Delta_i$; retain the best Δ_i.

$S(n) = \hat{P}_0/N_0$; current best SNR.

$\tau(n) = 7.5 + (80/\sqrt{S(n)})$; new time constant.

With a new value for $\mu_i(n)$ and $\tau(n)$, we can update coefficient $A_i(n)$ per Eq. (3), and therefore $W(k)$, per Eq. (1).

Step 5: The magnitudes of the Δ_i do not remain constant. They must diminish as the output power level $\hat{P}_0$ is driven toward the receiver noise level; otherwise the modulation perturbations will overdrive the desired null conditions and result in poor convergence behavior. The following logic procedure is used to continue from Step 4.

$$X = 7.5/\tau(n) \qquad\qquad \text{; dependence on current best SNR.}$$

$$Y = 10 * ALOG10 \ (Z) \qquad \text{; power level in dB.}$$

$$B = 10/(Y + 10) \qquad\qquad \text{; dependence on power level drop.}$$

$$Q = 0.022 * X * B \qquad\qquad \text{; maximum allowable value.}$$

$$DO\ 20\ J = 1,\ I$$

$$IF\ (Q > \Delta_i)\ GO\ TO\ 20$$

$$\Delta_i = Q \qquad\qquad\qquad \text{; reset } \Delta_i \text{ to new lower value.}$$

20   CONTINUE

Note that since $\hat{P}_0$ depends on all source nulling, then all Δ_i are set equal except for retention of a smaller prior value. This permits a ratchet-down convergence behavior.

Step 6:   If a given source is already in a sidelobe null, then the flag $(F = 1)$ set in Step 4 is used to bypass any change in the A_i coefficients of Eqs. (1) and (3). However, the modulation magnitude Δ_i for that particular source is reduced recursively to a very small value, essentially deleting it from the processing. The Fortran IV software logic statement entered from Step 4 is as follows:

33      $IF\ (F = 1)\ \Delta_i = 0.5 * \Delta_i + 0.00035$

In this statement, the value of Δ_i is reduced by 6 dB on each flag $(F = 1)$ recursion, reaching an ultimate minimum of -63 dB, if the source continues to remain in a sidelobe null.

Step 7:   If a given emitter happens to turn off, this would be detected by the source tracking/estimation subsystem, and it would soon be deleted from the high-priority source directory kept in memory. Thus, no further beam modulations would be made in its direction.

2.1 Modifications for Phase-Only Nulling

The algorithm described incorporates both amplitude and phase in the weight perturbations and will result in the best overall nulling performance. However, most phased array applications would require restriction of the perturbations to phase-only changes, so we introduce the modifications described here.

First, with reference to the vector diagram of Fig. 8, only the phase angle change is applicable so that Eq. (1) becomes,

13

$$W(k) = W_q(k) \left[1 + j \sum_{i=1}^{I} A_i \sin (\psi_i(k)) \right] \qquad (7)$$

where it is noted that only the imaginary part of the A_i terms is utilized. This permits us to understand the interesting phenomenon of unwanted "symmetrical lobes" that appear in phase-only modulation, because we can substitute the following trigonometric identity into Eq. (7),

$$j \sin (\psi_i(k)) = \frac{1}{2} [e^{j\psi_i(k)} - e^{-j\psi_i(k)}]. \qquad (8)$$

Obviously, we have two lobes located at $\pm \psi_i(k)$, and from Eq. (2) we see that they are symmetrical with respect to the pointing direction of the mainbeam. An example pattern plot of such lobes is discussed in Section 3.

Equations (2) through (4) remain unchanged, but in Step 2 it is necessary to double the initial value for the weight perturbation magnitudes Δ_i. For the example given, we now set all $\Delta_i = 0.034$, or -30 dB level. The reason for doubling is that phase-only modulation is roughly half as effective as the combined amplitude plus phase.

In Step 3, we again encounter the phase angle restriction so that Eqs. (5) and (6) become

$$W_i^+(k) = W(k) [1 + j\Delta_i \sin (\psi_i(k))], \text{ and} \qquad (9)$$

$$W_i^-(k) = W(k) [1 - j\Delta_i \sin (\psi_i(k))]. \qquad (10)$$

Steps 4 and 5 remain the same, but in Step 6 we again double the minimum modulation value for the flag ($F = 1$) condition,

33 IF ($F = 1$) $\Delta_i = 0.5 * \Delta_i + 0.0007$

such that the ultimate minimum value is now -57 dB if the source continues to remain in a sidelobe null.

2.2 Other Algorithms

The algorithm just described is a beamspace, single-cycle, plus-minus perturbation sequence technique that uses the changes in smoothed/averaged output power. There are also other algorithms and techniques described in the literature that would be suitable for our application. For example, the orthogonal binary code sequences described by Cantoni and Godara [19,20] could be adapted to our situation, where it is noted that they correlate the instantaneous output power with their sequences rather than the smoothed output power. Also, the coherent perturbation-algorithm work of Davis et al. [21] should be applicable. These other techniques are not pursued in this investigation.

3.0 SIMULATION RESULTS FROM APERTURE-RIPPLE ALGORITHM

In this section, we describe performance results obtained by applying the algorithms of Section 2 to computer-simulated source situations. Figure 9(a) illustrates an example wherein we have two rather strong emitters of 46 dB SNR located in the sidelobe region of a 16 element linear array with

14
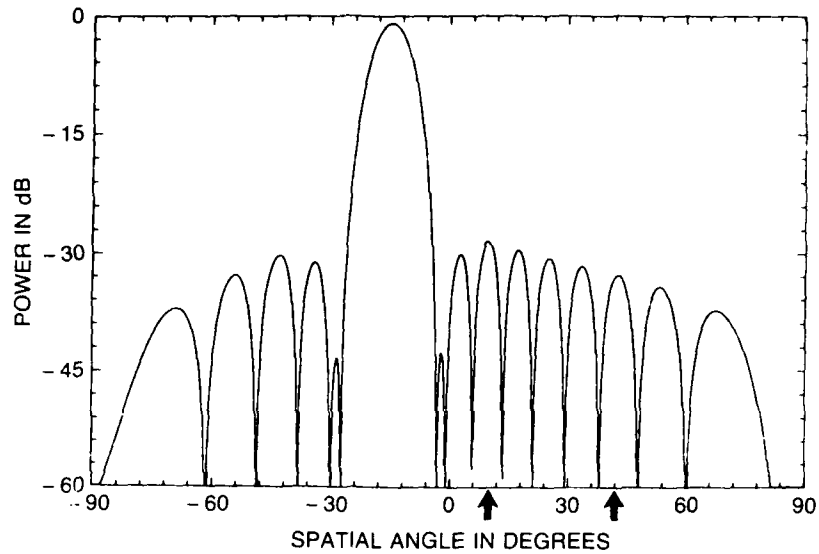
(a)
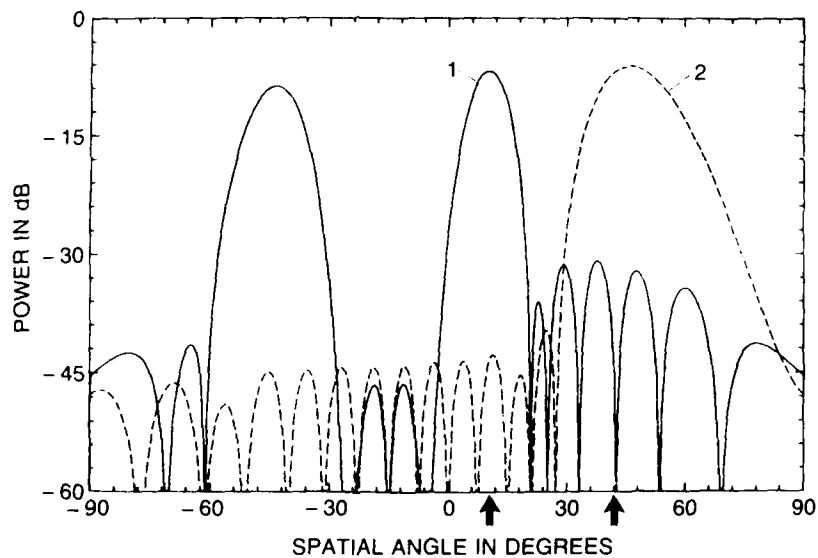
(b)

Fig. 9 — Quiescent mainbeam and aperture ripple-modulation beams for 16 element
linear array, two 46 dB sources at 10° and 42°; (a) quiescent mainbeam pattern, 30
dB Taylor weighting, and (b) subtraction beams resulting from phase-only
perturbation

half-wavelength element spacing, and a 30 dB Taylor illumination. The sources are noncoherent and
are swept in frequency over a 5% RF bandwidth. Since we know the directions of the sources, phase
perturbations are applied across the array to generate two beams in those directions. Figure 9(b)
illustrates pattern plots of the two beams, labelled 1 and 2; note that these beams are the result of
phase-only perturbation. They have good sidelobe levels because they automatically incorporate the
30 dB taylor illumination taper, but they are also subject to the appearance of unwanted "symmetrical
lobes" because of the phase-only approximation discussed in Section 2.

The symmetrical lobe appears on the opposite side of the mainbeam, i.e., the mainbeam pointing direction is the point of symmetry as seen in Fig. 9 for the Number 1 beam. Note in Fig. 9 that the symmetrical lobe for the Number 2 beam does not appear in visible space because it is too far beyond the mainbeam direction. If the perturbations were to incorporate both amplitude and phase, then the unwanted symmetrical lobes would not be formed.

As discussed in section 2, the search algorithm applies a starting perturbation magnitude level that is roughly equal to the mainbeam sidelobe level, and it monitors the averaged power output for a plus-minus sequence modulation. If the power output drops below the $\hat{P}_0$ level as measured on the previous trial, that perturbation is retained and the value of $\hat{P}_0$ is reset to the new lower level. Figure 10(a) shows the resultant "ratchet-down" effect on the output power level, where it is noted that convergence occurs in about 600 "snapshots" for this case.

A snapshot is equivalent to the element data contained in one range bin sampled simultaneously across the array [4]. In Fig. 10, the dot symbol "." denotes the instantaneous power output of the mainbeam from each snapshot; the clusters of " + " symbols denote an average of the instantaneous power taken over the previous 21 snapshots; they clearly identify the $\hat{P}_i^{(+)}$ and $\hat{P}_i^{(-)}$ power levels associated with a given weight perturbation. The horizontal line symbols "_____" denote the unperturbed average power level $\hat{P}_0$ from the previous plus-minus perturbation sequence; the heavy, dashed-line has been added to allow the reader to follow the approximate convergence of the average output power level down to receiver noise level (0 dB).

The reader may find it helpful to go through the first complete plus-minus sequence indicated in Fig. 10(a). Starting from the left, the initial new start $\hat{P}_0$ unperturbed level is about 29.5 dB. The first plus-minus cycle is then directed toward source Number 1 located at $+10°$ azimuth; the resultant power levels are identified as $\hat{P}_1(+)$ at 28.5 dB and $\hat{P}_1(-)$ at 33.5 dB, from which the (+) perturbation is retained and $\hat{P}_0$ is reset to equal $\hat{P}_1(+)$ at 28.5 dB. The second plus-minus cycle is then directed toward source Number 2 located at $+42°$ azimuth; the resultant power levels are identified as $\hat{P}_2(+)$ at 26 dB and $\hat{P}_2(-)$ at 29 dB, from which the (+) perturbation is retained and $\hat{P}_0$ is reset to equal $\hat{P}_2(+)$ at 26 dB. The sequence is then repeated until the output converges close to the receiver noise power level. Figure 10(b) illustrates the somewhat faster convergence obtained when the perturbations incorporate both amplitude and phase.

Figure 11 shows a typical adapted pattern after convergence. The adapted pattern remains quite stable and has successfully nulled out both sources. A modest increase in a sidelobe can be seen on the left-hand side of the mainbeam at about $-44°$, which is the exact position of the unwanted symmetrical lobe discussed in Fig. 9(b).

4.0 BEAMSPACE TECHNIQUES FOR IMPROVING PERFORMANCE

Thus far, we have considered only the most simple configuration where there is just one mainbeam output port to work with. In this Section we discuss the concept of having available additional output-beam ports. For example, let us assume that our phased-array antenna system has monopulse tracking capability with both a sum (Σ) and a difference (Δ) output port, as shown in Fig. 12. This constitutes an advantage for our simple adaptive system because the availability of any extra beam port essentially gives us an auxiliary beam, an extra DOF. Because of this, several different ways exist for improving our adaptive performance.

First, one could simply apply the aperture ripple modulation technique of Section 2 separately to the Σ and Δ beams. This would require superposition of the two modulations of each element weight, but the fact that the Σ and Δ beams are orthogonal (or nearly so) should permit the technique

16
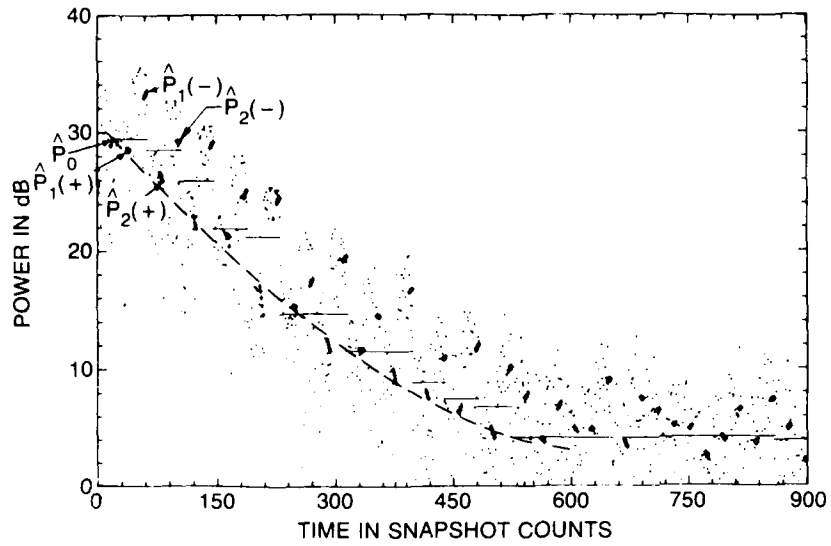
(a)
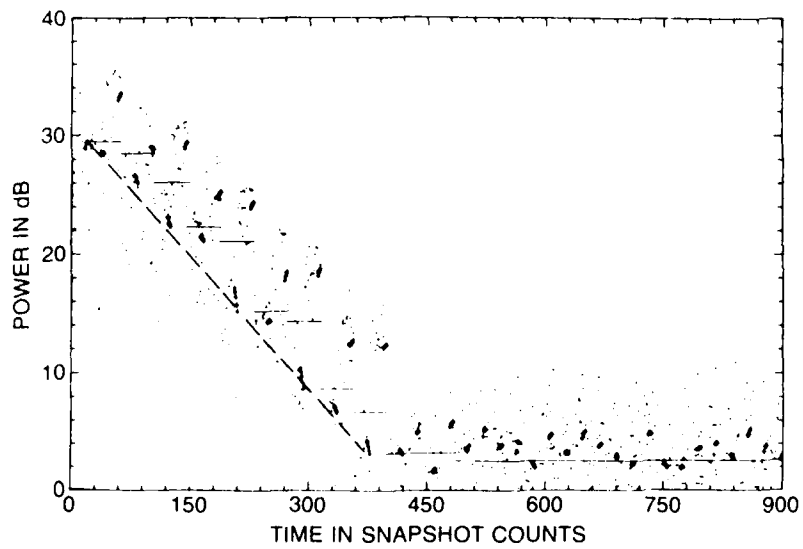
(b)

Fig. 10 — Convergence response performance for beamspace, single-cycle, plus-minus perturbation sequence search algorithm. Processed for two-source case of Fig. 9. (a) phase-only (phase shifter) perturbation, and (b) amplitude and phase weight perturbation.
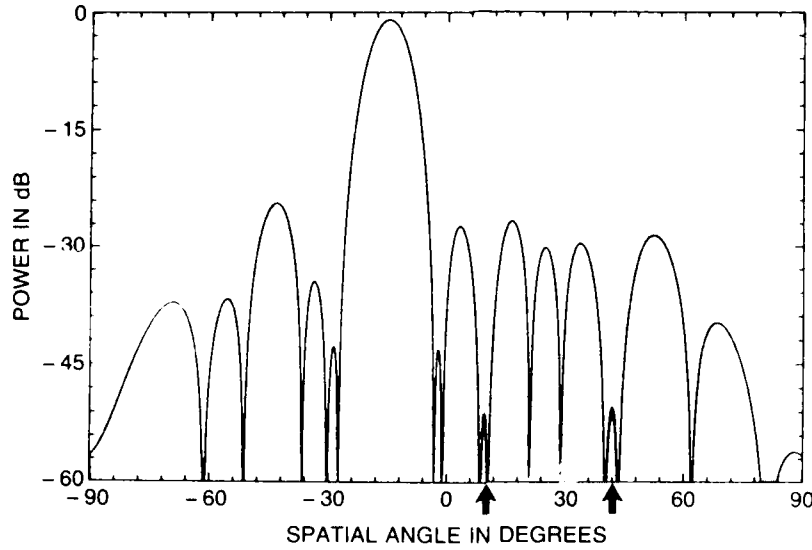
Fig. 11 — Adapted pattern after convergence for the two-source case
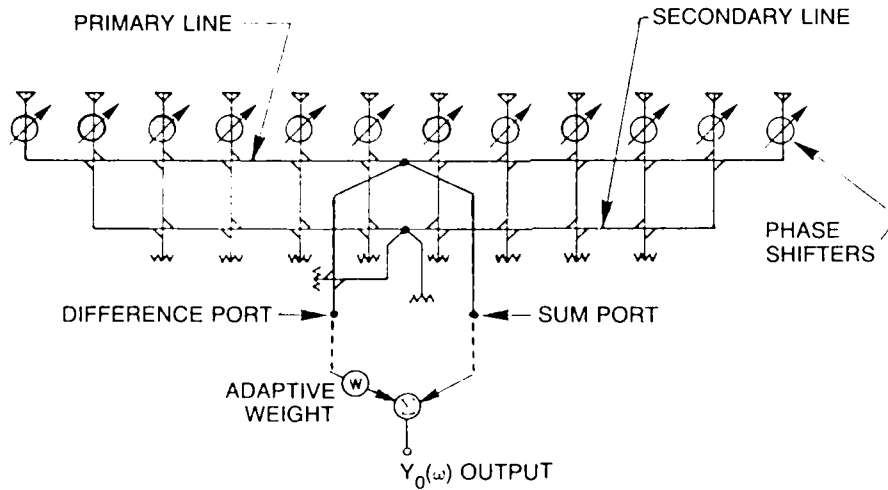of Fig. 9; five independent trials plotted

Fig. 12 — Typical monopulse sum and difference beamformer network, with
adaptive weight option added for using the difference beam as an auxiliary

to develop overlapping nulls in the two patterns. Alternatively, we could work with the two halves of the array before the signals are combined into the Σ and Δ channels. Haupt [22] discusses the ramifications of simultaneous nulling in Σ and Δ channels.

Second, by reserving the Δ beam for use as an auxiliary canceller beam, one can separate the steering of a low-level lobe toward an emitter from the adaptive weight needed to subtract it from the Σ beam. This option is indicated by the dashed-line configuration in Fig. 12, and it would have the advantage of very fast cancellation for a single interference source. The disadvantages to the option include rather large changes in the resultant adapted Σ pattern: not only are there sidelobe perturbations in the vicinity of the emitter, but the mainlobe suffers distortion because of the subtraction of the Δ beam from it. Note that this option results in the interesting phenomenon that a "Σ type" of ripple beam exists in the Δ channel, and a "Δ type" of ripple beam exists in the Σ channel.

Next, let us assume that our phased-array antenna system consists of a space-fed lens in which the mainbeam is scanned by phase-shifters located in the objective lens, and we wish to consider the option of using an off-axis, defocused feed as an auxiliary beam. Figure 13 illustrates this configuration. The possibility here is that aperture ripple modulation could be used to focus the defocused feed onto the emitter, and then adaptively weight its output to cancel the interference from the mainbeam. Again, this configuration would have the advantage of separating the steering of a low-level lobe from its adaptive weight and could achieve very fast cancellation of the interference source. Some deterioration in the resultant adapted pattern sidelobes should be expected because of the double defocusing action, i.e., the mainbeam sidelobes will be perturbed by the defocused aperture ripple, and the defocused feed will have a "major lobe" caused by "looking thru" the mainbeam focusing. This major lobe appears in the sidelobes of the resultant adapted pattern. Note that linear superposition allows us to add several defocused feeds to this type of phased-array system, thus making it amenable to very fast adaptive response with several DOF.
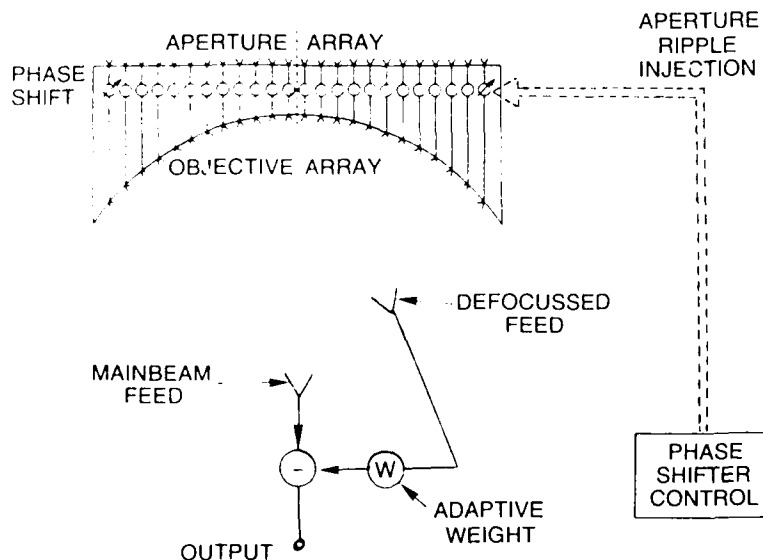

Fig. 13 — Space-fed lens configuration utilizing off-axis, defocused feed to obtain an auxiliary beam for sidelobe nulling

5.0 CONCLUSIONS

Several simple phase-shifter nulling techniques have been investigated for application to large-aperture phased arrays. The intended purpose is to provide a modest partial adaptive capability at reasonable cost. These techniques depend on having access to the array-element phase shifters for the injection of small phase (and/or amplitude) perturbations of the mainbeam aperture distribution, but they do not require auxiliary elements, correlators, or beam-formers. A key factor to their successful operation is a priori knowledge of the directions/locations of emitter sources to be nulled out, and this must be provided for either by mainbeam tracking of the sources or by a separate source estimation processor subsystem.

A complete description is given for the particular aperture ripple modulation algorithms used, based on beamspace decomposition and adaptive "search" techniques. These algorithms are then applied to a computer-simulated source situation involving two strong noncoherent emitters that are swept in frequency over a 5% bandwidth. Both sources are nulled out within about 600 snapshots of data, which is a remarkably fast convergence for such a simple phase-only adaptive system. The performance results achieved indicate that the concept is feasible and should be investigated further in an experimental phased-array system. Some additional beamspace options are also described, which would permit improvements in adaptive performance if additional DOF were available.

6.0 REFERENCES

1. H.L. Southall and D.T. McGrath, "An Experimental Completely Overlapped Subarray Antenna," *IEEE Trans. Antennas Propag.* **AP-34**, 465-474 (1986).

2. P.W. Howells, "Explorations in Fixed and Adaptive Resolution at GE and SURC," *IEEE Trans. Antennas Propag.* **AP-24**, 574-584 (1976).

3. S.P. Applebaum, "Adaptive Arrays," *IEEE Trans. Antennas Propag.* **AP-24**, 585-598 (1976).

4. W.F. Gabriel, "Using Spectral Estimation Techniques in Adaptive Processing Antenna Systems," *IEEE Trans. Antennas Propag.* **AP-34**, 291-300 (1986).

5. J.T. Mayhan, "Adaptive Nulling with Multiple-Beam Antennas," *IEEE Trans. Antennas Propag.* **AP-26**, 267-273 (1978).

6. R.N. Adams, L.L. Horowitz, and K.D. Senne, "Adaptive Main-Beam Nulling for Narrow-Beam Antenna Arrays," *IEEE Trans. Aerospace Electron. Syst.* **AES-16**, 509-516 (1980).

7. S.P. Applebaum and D.J. Chapman, "Adaptive Arrays with Mainbeam Constraints," *IEEE Trans. Antennas Propag.* **AP-24**, 650-662 (1976).

8. D.J. Chapman, "Partial Adaptivity for the Large Array," *IEEE Trans. Antenna Propag.* **AP-24**, 685-696 (1976).

9. R.L. Fante, "Systems Study of Overlapped Sub-Arrayed Scanning Antennas," *IEEE Trans. Antennas Propag.* **AP-28**, 668-679 (1980).

10. E.C. DuFort, "An Adaptive Low-Angle Tracking System," *IEEE Trans. Antennas Propag.* **AP-29**, 766-772 (1981).

11. E.C. DuFort, "An Optical Subarray Antenna Having Antenna Nulling Applications," *IEEE Trans. Antennas Propag.* **AP-35**, 643-651 (1987).

12. C.A. Baird and G.G. Rassweiler, "Adaptive Sidelobe Nulling Using Digitally Controlled Phase-Shifters," *IEEE Trans. Antennas Propag.* **AP-24**, 638-649 (1976).

13. E.T. Ozaki et al., "An Experimental Adaptive Null Steering Array Using a Phase-Only Pattern Search Algorith," Proceedings of the Phased Arrays 1985 Symposium, RADC Report TR-85-170, Sept. 1985.

14. R.S. Chu et al., "An Adaptive Null Steering Study Using Transform Feed," Proceedings of the Phased Arrays 1985 Symposium, RADC Report TR-85-170, Sept. 1985.

15. W.F. Gabriel, "Constrained Beamspace Sidelobe Canceller (SLC) with a Tapped Delay Line on Each Beam," NRL Memorandum Report 6042, Sept. 1987.

16. R.A. Monzingo and T.W. Miller, *Introduction to Adaptive Arrays* (John Wiley and Sons, New York, 1980).

17. W. Rotman and R.F. Turner, "Wide-Angle Microwave Lens for Line Source Application," *IEEE Trans. Antennas Propag.* **AP-11**, 623-632 (1963).

18. M.I. Skolnik, *Radar Handbook* (McGraw-Hill, New York, 1970). (Reference Chapter 11, T.C. Cheston and J. Frank, PP. 11-39 to 11-43.)

19. A. Cantoni, "Application of Orthogonal Perturbation Sequences to Adaptive Beamforming," *IEEE Trans. Antennas Propag.* **AP-28**, 191-202 (1980).

20. L.C. Godarda and A. Cantoni, "Analysis of the Performance of Adaptive Beamforming Using Perturbation Sequences," *IEEE Trans. Antennas Propag.* **AP-31**, 268-279 (1983).

21. R.M. Davis, O.C. Farden, and P.J. Sher, "A Coherent Perturbation Algorithm," *IEEE Trans. Antennas Propag.* **AP-34**, 380-387 (1986).

22. R.L. Haupt, "Simultaneous Nulling in the Sum and Difference Patterns of a Monopulse Antenna," *IEEE Trans. Antennas Propag.* **AP-32**, 486-493 (1984).